Supplementary materials

Comet assay

The generation of DNA strand breaks was assessed by single cell gel electrophoresis (Comet) assay (1), using a Fpg-FLARE (Fragment length analysis using repair enzymes) comet kit in accordance with the manufacturer's instructions (Trevigen, Cat # 4250-050-K, Gaithersburg, MD). For each experimental points at least three different mice were analyzed, and 50 cells were evaluated from each experiment. Comet tail length and tail moment were measured under a fluorescence microscope (Zeiss AXIO Imager 72) using an automated image analysis system based on a public domain NIH Image Program.

Flow cytometry analysis for DDR signatures and phosphorylated p65

DDR signature and phosphorylated p65 staining were performed after fixation and permealibization using Cytofix/Cytoperm buffer (BD PahrMingen, Cat # 554722, San Jose, CA) and washed using Perm/Wash Buffer (BD PharMingen, Cat # 554723, San Jose, CA). Cells were then incubated with antibodies against p53-S15 (Cell Signaling Tech, Cat # 9284, Danvers, MA), ATM-S1981 (BioLegend, Cat # 651204, San Diego, CA), and CHK2-T68 (eBioscience, Cat # 12-9508-41, Waltham, MA), or phosphor-p65 (Ser536) (ref. 2, 3, Cell Signaling Tech, Cat # 5733S, Danvers, MA), respectively.

Supplementary references

1. Li X, Sipple J, Pang Q, Du W. Salidroside stimulates DNA repair enzyme Parp-1 activity in mouse HSC maintenance. *Blood.* 2012;119(18):4162-4173.
2. Maguire O, O'Loughlin K, Minderman H. Simultaneous assessment of NF-κB/p65 phosphorylation and nuclear localization using imaging flow cytometry. *J Immunol*. Methods. 2015;423:3-11.
3. Kwon HJ, et al. Stepwise phosphorylation of p65 promotes NF-κB activation and NK cell responses during target cell recognition. *Nat Commun.* 2016;7:11686.

Supplementary Table

Table S1. Primers used for qPCR analysis

Gene	Forward	Reverse
Nlrp12	TGATGAACAGGATCTTGGGA	TGGAAACTCAGGTGGATGAA
IL-1β	CCTTCCAGGATGAGGACATGA	TGAGTCACAGAGGATGGGCTC
IL-6	GAGGATACCACTCCCAACAGACC	AAGTGCATCATCGTTGTTCATACA
Eya2	TCGGGACGACTCTGCACTGT	GCTGTACTGTGTCTGGCCATAGG
Gapdh	TCAATGAAGGGGTCGTTGAT	CGTCCCGTAGACAAAATGGT
NLRP12	CAGGCATGATGCTGCTTTGCGA	AGCACAGAAGCCATCTCCTGAC
FANCA	CCA AGG CCA TGT CCG ACT CG	CAG AAA GCA TGG CCC TGG CGA CG
GAPDH	GTCTCCTCTGACTTCAACAGCG	ACCACCCTGTTGCTGTAGCCAA

Supplementary figures

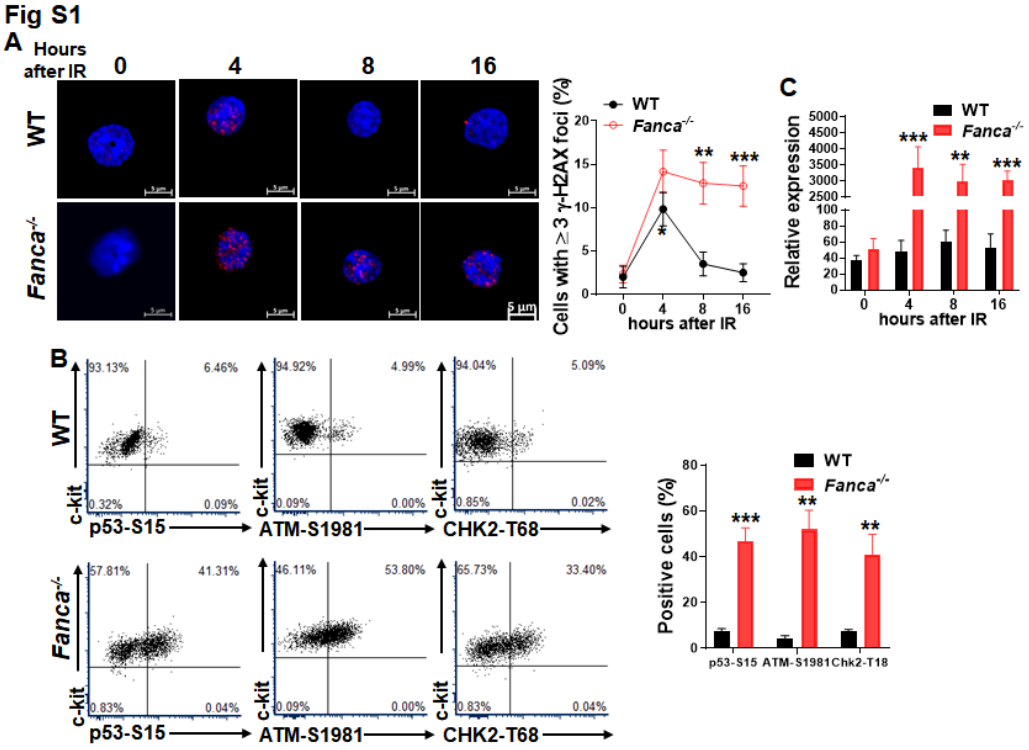

Fig S1. Persistent DNA damage induces *Nlrp12* upregulation in *Fanca*$^{-/-}$ HSCs. (A) Persistent DNA damage-induced by ironizing radiation (IR) in *Fanca*$^{-/-}$ HSCs. *Fanca*$^{-/-}$ mice and their wild-type (WT) littermates were irradiated with 500 cGy of TBI. Bone marrow (BM) SLAM (Lin^{-}Sca1^{+}c-kit^{+}CD150^{+}CD48^{+}) cells were isolated at the indicated timepoints post-IR and subjected to immunofluorescence staining for γ-H2AX. Representative images (Left) and quantification (Right) of γ-H2AX foci forming kinetics are shown. 0h, untreated control (n=6 per group). (B) IR-induced activation of DNA damage response (DDR) in *Fanca*$^{-/-}$ HSCs. *Fanca*$^{-/-}$ mice and their WT littermates were irradiated with 500 cGy of TBI. BM SLAM cells were isolated at the indicated timepoints post-IR and subjected to flow cytometry analysis for phosphorylation of ATM-S1981, CHK2-T68 and p53-S15. Representative flow plots at 8 hours post-IR (Left) and

quantifications of DDR kinetics (Right) are shown (n=6 per group). (C) Persistent DNA damage-induced *Nlrp12* expression in *Fanca*$^{-/-}$ HSCs upon IR. *Fanca*$^{-/-}$ mice and their WT littermates were irradiated with 500 cGy of TBI. BM SLAM cells were isolated at the indicated timepoints post-IR and subjected to qPCR analysis for *Nlrp12* expression using primers listed in Table S1. Samples were normalized to the level of *GAPDH* mRNA (n=6 per group).

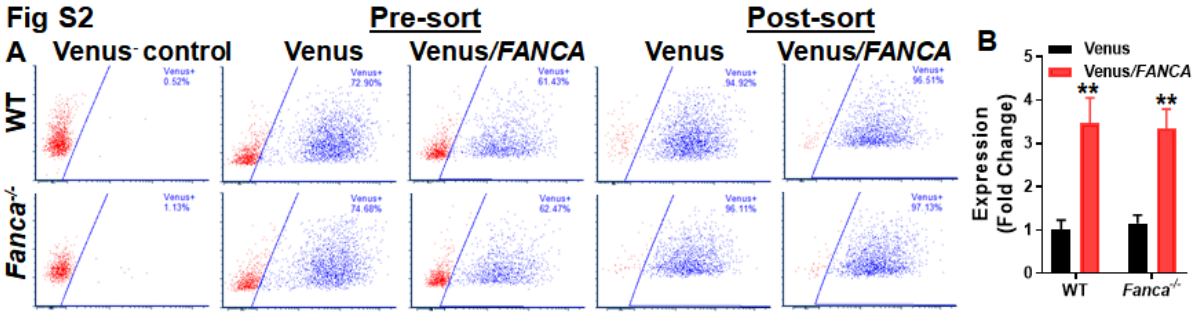

Fig S2. Transduction efficiency and FACS of lentiviral vector expressing Venus and *FANCA*. Bone marrow (BM) LSK (Lin$^-$Sca1$^+$c-kit$^+$) cells from *Fanca*$^{-/-}$ mice and their WT littermates were transduced with lentiviral vector expressing Venus or Venus/FANCA. (A) Representative flow plots of pre- and post-cell sort are shown. (B) The transduced cells in (A) were subjected to qPCR analysis for *FANCA* expression using primers listed in Table S1. Samples were normalized to the level of *GAPDH* mRNA.

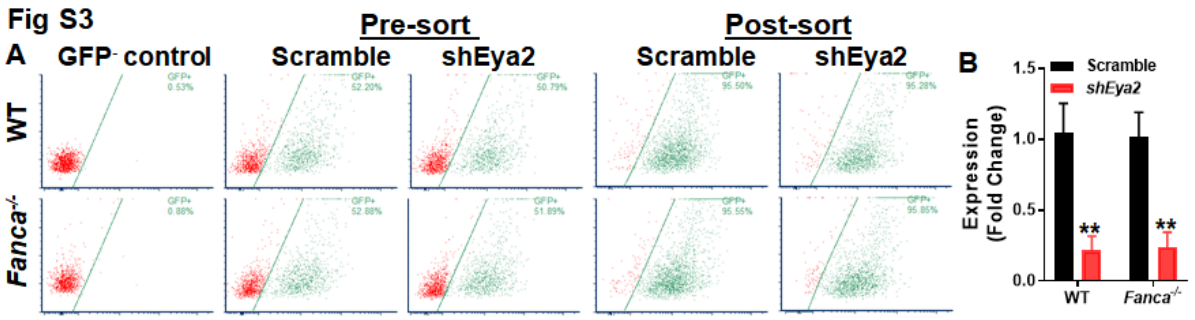

Fig S3. Transduction efficiency and FACS of lentiviral vector expressing Scramble shRNA or shRNA targeting *Eya2*. BM LSK ($Lin^{-}Sca1^{+}c\text{-}kit^{+}$) cells from WT mice were transduced with lentiviral vector expression Scramble shRNA or shRNA targeting *Eya2*. (A) Representative flow plots of pre- and post-cell sort are shown. (B) The transduced cells in (A) were subjected to qPCR analysis for *Eya2* expression using primers listed in Table S1. Samples were normalized to the level of *GAPDH* mRNA.

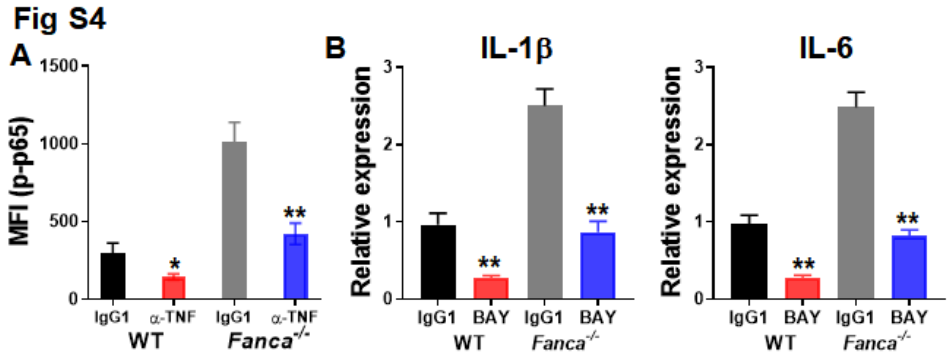

Fig S4. TNF neutralization or NF-κB inhibition suppresses downstream signaling. **(**A) Inhibition of NF-κB activation by anti-TNFα neutralizing antibody. WBMCs from mice treated with anti-TNFα neutralizing antibody or IgG1 control, as described in Figure 2H-I, were subjected to flow cytometry analysis for phosphorylated p65 (p-p65) in SLAM cells. (B) BAY11-7082 suppresses *IL-1β* and *IL-6* expression. RNA were extracted from WBMCs from mice injected with BAY11-7082 or IgG1 control, as described in Figure 2H-I, followed by qPCR analysis for *IL-1β* and *IL-6* expression using primers listed in Table S1.

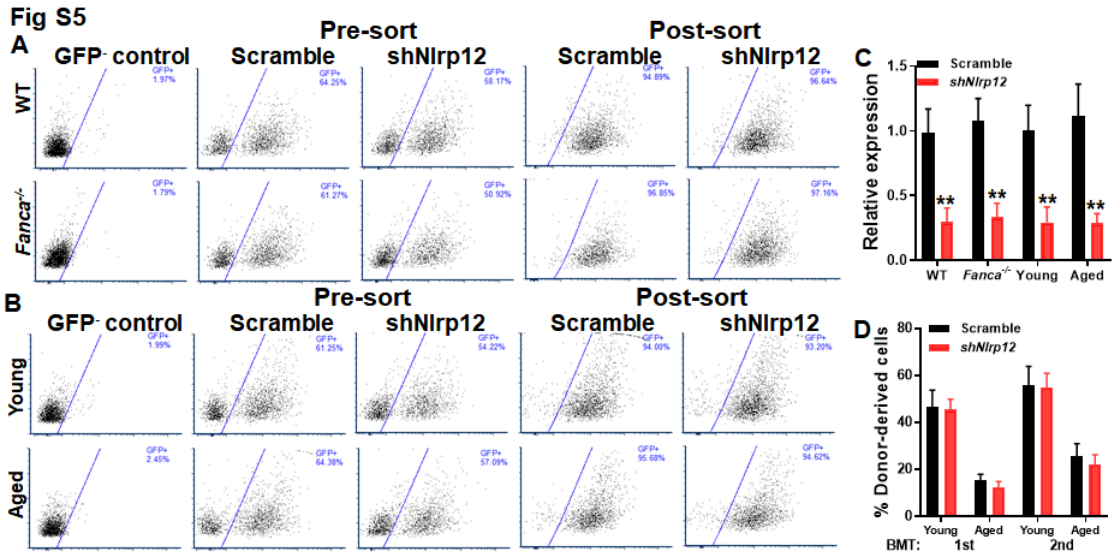

Fig S5. Transduction efficiency and FACS of lentiviral vector expressing Scramble shRNA or shRNA targeting *Nlrp12*. BM LSK (Lin$^-$Sca1$^+$c-kit$^+$) cells from *Fanca*$^{-/-}$ mice and their WT littermates (A), or young and aged mice (B) were transduced with lentiviral vector expression Scramble shRNA or shRNA targeting *Nlrp12.* Representative flow plots of pre- and post-cell sort are shown. (C) The transduced cells in (A and B) were subjected to qPCR analysis for *Nlrp12* expression using primers listed in Table S1. Samples were normalized to the level of *GAPDH* mRNA. (D) Depletion of Nlrp12 compromises HSC function in aged mice. LSK cells from young or aged mice were transduced with lentiviral vector expressing scramble shRNA or shRNA targeting *Nlrp12*. 2,000 sorted GFP$^+$ cells, along with 2X10^5 protector cells, were transplanted into lethally irradiated BoyJ recipients. Donor-derived chimera in primary recipients (Left) or secondary recipients (Right) were determined by flow cytometry at 16 weeks post-transplant (n=9-12).

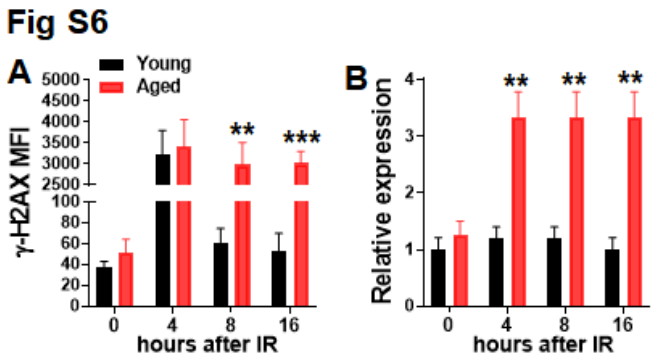

Fig S6. IR-induced persistent DNA damage and *Nlrp12* upregulation in aged HSCs. (A) IR-induced persistent DNA damage in aged HSCs. Young and aged mice were irradiated with 500 cGy of TBI. BM SLAM cells were isolated at the indicated timepoints post-IR and subjected to flow cytometry analysis for γ-H2AX (n=6 per group). (B) Persistent DNA damage-induced *Nlrp12* expression in aged HSCs upon IR. Young and aged mice were irradiated with 500 cGy of TBI. BM SLAM cells were isolated at the indicated timepoints post-IR and subjected to qPCR analysis for *Nlrp12* expression using primers listed in Table S1. Samples were normalized to the level of *GAPDH* mRNA (n=6 per group).

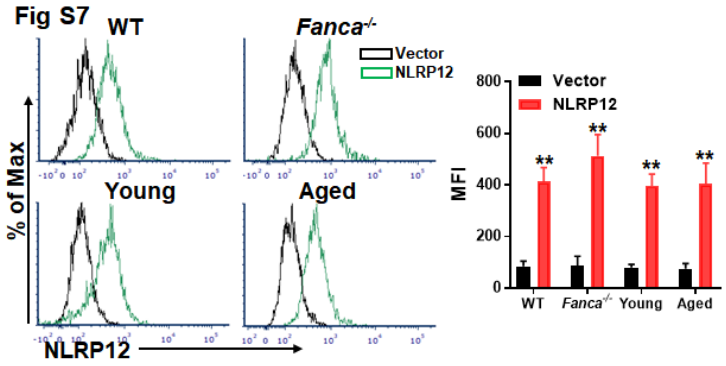

Fig S7. Ectopic expression of Nlrp12 in transduced cells. BM LSK cells from *Fanca*$^{-/-}$ mice or their WT littermates (Upper), or young and aged mice (Lower) were transduced

with lentiviral vector expressing eGFP vector only or eGFP/Nlrp12. 2,000 GFP^+ sorted cells, along with $2X10^5$ protector cells, were then transplanted into lethally irradiated BoyJ recipients. Donor-derived HSCs ($GFP^+CD45.2^+Lin^-c\text{-}kit^+Sca1^+CD150^+CD48^-$) from the recipients were subjected to flow cytometry analysis for NLRP12. Representative flow plots (Left) and quantification of mean fluorescence intensity (MFI; Right) are shown (n=9).

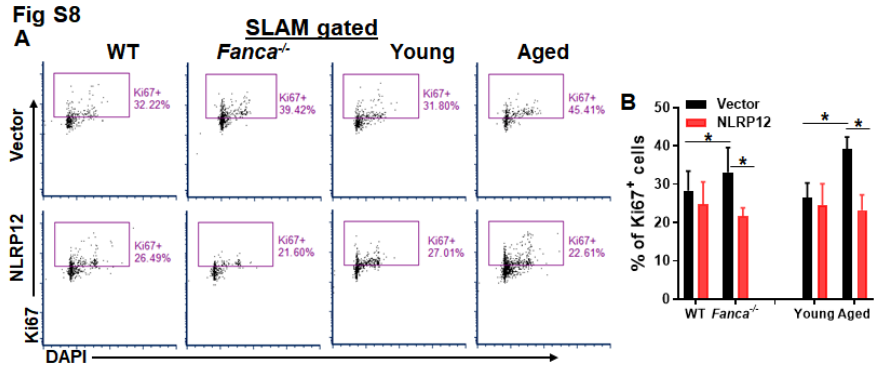

Fig S8. NLRP12 increases quiescence of *Fanca*$^{-/-}$ and aged HSC. LSK cells from WT and *Fanca*$^{-/-}$ mice, or young and old mice were transduced with lentiviral vector expressing eGFP-alone (Vector) or eGFP-*NLRP12*. 2,000 sorted cells, along with $2X10^5$ protector cells, were transplanted into lethally irradiated BoyJ recipients. 16 weeks post-transplant, BM WBMCs were subjected to Flow cytometry analysis for cell cycle in donor-derived SLAM cells using anti-Ki67 antibody and DAPI. Representative flow plots (Left) and quantification (Right) are shown (n=9 per group).

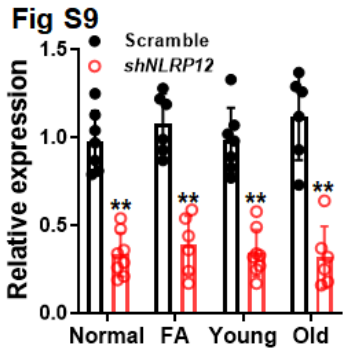

Fig S9. NLRP12 knockdown in human samples. BM CD34$^+$ cells from healthy donors (Normal) and FA patients; or young and aged donors were transduced with lentiviral vector expression Scramble shRNA or shRNA targeting human *NLRP12* followed by cell sorting for GFP. RNA were extracted from the sorted GFP$^+$ cells for quantitative RT-PCR analysis using primers listed in Table S1. Levels of the expression in each sample were normalized to the level of *GAPDH* mRNA (n=6-8).